

# Inverse Hasimoto Map and Deformed Nonlinear Schrödinger Equation

Kumar Abhinav<sup>1\*</sup> and Partha Guha<sup>2†</sup>

<sup>1</sup>The Institute for Fundamental Study (IF), Naresuan University,  
Phitsanulok 65000, Thailand

<sup>2</sup>S. N. Bose National Centre for Basic Sciences,  
JD Block, Sector III, Salt Lake, Kolkata - 700098, India.

December 20, 2024

## Abstract

A mapping from the solutions of vortex filament equation in the Local Induction Approximation (LIA) to soliton solutions of the NonLinear Schrödinger equation was obtained by Hasimoto [R. Hasimoto, J. Fluid Mechanics **51**, (1972) 477]. We utilize it to obtain an Inverse Hasimoto Map from the single soliton solution of the nonlinear Schrödinger equation to the propagating three-dimensional parametric curve governed by Frenet-Serret equation. Further, the effects of quasi-integrable and non-holonomic deformations in the solitonic sector are obtained as particular modification (or lack thereof) to the corresponding curve evolution. In other words, we compute the motion of position vector of generalized vortex filament equation from the solution of the generalized nonlinear Schrödinger equation. This inverse Hasimoto map can be a geometrical tool to analyze localized evolution of dynamics in various dynamical systems.

**Mathematics Subject Classifications (2010):** 35Q55, 37K10, 37K25, 37K55.

**Keywords and Keyphrases.** Nonlinear Schrödinger equation, Inverse Hasimoto Map, Quasi-integrable deformation, Non-holonomic deformation, Solitons.

## 1 Introduction

Evolution of systems like Vortex filaments in perfect fluids and one-dimensional classical continuum Heisenberg spin chain [1] may mathematically be modelled as a moving space curve  $\gamma(s, t) \subset \mathbb{R}^3$ . Da Rios [2] derived a set of two coupled equations governing the in-extensional motion of a vortex filament within an irrotational fluid in terms of time evolution of its intrinsic geometric parameters: curvature ( $\kappa(s, t)$ ) and torsion ( $\tau(s, t)$ ), which were rediscovered by Betchov decades later [3].

Hasimoto showed that the Da RiosBetchov equations,

$$\kappa_t + 2\tau\kappa_s + \tau_s\kappa = 0 \quad \text{and} \quad \tau_t + \left(\tau^2 - \frac{1}{2}\kappa^2 - \frac{\kappa_{ss}}{\kappa}\right)_s = 0 \quad (1)$$

can elegantly be combined to give a focusing-type nonlinear Schrödinger (NLS) equation [4],

$$q_t - iq_{ss} - 2i\eta|q|^2q = 0, \quad (2)$$

---

\*E-mail: kumara@nu.ac.th

†E-mail: partha@bose.res.in

using the so called Hasimoto map [5]:

$$q(s, t) = \kappa(s, t) \exp \left\{ i \int_{-\infty}^s \tau(s', t) ds' \right\}, \quad (3)$$

relating the Frenet-Serret space-time parameters  $\tau(s, t)$  and  $\kappa(s, t)$  to the NLS amplitude  $q(s, t)$ . Interestingly the characteristics of the NLS system like energy and momentum densities,  $\kappa^2$  and  $\kappa^2\tau$  respectively, are directly given by the geometric parameters. The non-linear coupling  $\eta$  directly reflects the on-site interaction strength of the physical system. These equations prescribe (up to a rigid motion) the evolution of a vortex filament in an infinite domain of  $\mathbb{R}^3$  for given initial conditions  $\kappa(s, 0)$  and  $\tau(s, 0)$ . Correspondingly the single-soliton solution of this equation describes a *isolated loop* of helical twisting motion along the vortex line [6].

In this work we seek to realize the Frenet-Serret curve dynamics as a direct demonstration of particular solutions of the NLS system. Particularly, solitonic NLS solutions are of both mathematical and physical interest including their certain classes of deformations, namely quasi-integrable (QI) [7, 8] and non-holonomic (NH) [9, 10, 11] ones. In addition to the formal interest, such a venture should yield crucial understanding of physical systems (*e. g.* spin configuration, filament dynamics in fluids etc.) that can effectively be represented by localized solutions, and by their subsequent deformations, in the NLS sector. It can further shed light on stability or lack thereof of a particular physical state based on properties of the corresponding nonlinear solution. Such correspondence between physical systems and NLS systems [12, 13] with subsequent deformations [14] have been studied before. Much wider implications could be in case of NLS (and derivative NLS) hierarchies, whose QI and NH deformations are known [15].

Initial computation of an inverse Hasimoto transformation to reformulate the Da Rios-Betchov type equations have been studied by Sym [16] and Aref-Linchem [17]. In order to obtain the curve dynamics from a given solution of the NLS system we employ a somewhat straight-forward path that can be termed as the *inverse Hasimoto map* (IHM). Following Ref. [18] the Frenet-Serret equations can be cast into the matrix form:

$$\mathbf{W}_s = \mathcal{A}(s, t)\mathbf{W}, \quad (4)$$

where  $\mathbf{W} = [\mathbf{t} \ \mathbf{n} \ \mathbf{b}]^T$  and

$$\mathcal{A}(s, t) = \begin{bmatrix} 0 & \kappa(s, t) & 0 \\ -\kappa(s, t) & 0 & \tau(s, t) \\ 0 & -\tau(s, t) & 0 \end{bmatrix}. \quad (5)$$

Here the *parametric* space ( $s$ ) and time ( $t$ ) derivatives of the tangent ( $\mathbf{t}$ ), normal ( $\mathbf{n}$ ) and binormal ( $\mathbf{b}$ ) of a space-time curve are interrelated by its curvature ( $\kappa$ ) and torsion ( $\tau$ ). The Hasimoto map relates curvature and torsion to the amplitude  $\psi(s, t)$  of a certain dynamical equation. Thus the IHM amounts to solve for  $\mathbf{W}$  that in turn should yield the tangent ( $\mathbf{t}$ ). Since the latter is the derivative of the curve's coordinates  $\{x_i\}$  with respect to the space parameter  $s$ , a further integral yields the motion of the curve with time  $t$  as a parameter.

The solution for Eq. 4 has a general form [18]:

$$\mathbf{W}(s, t) = \exp[\mathcal{M}(s, t)] \mathbf{C}(t). \quad (6)$$

Herein,

$$\mathbf{M}(s, t) := \exp[\mathcal{M}(s, t)] = \begin{bmatrix} \frac{b^2}{c^2} + \frac{a^2}{c^2} \cos(c) & \frac{a}{c} \sin(c) & \frac{ab}{c^2} [1 - \cos(c)] \\ \frac{a}{c} \sin(c) & \cos(c) & \frac{b}{c} \sin(c) \\ \frac{ab}{c^2} [1 - \cos(c)] & \frac{b}{c} \sin(c) & \frac{a^2}{c^2} + \frac{b^2}{c^2} \cos(c) \end{bmatrix}, \quad (7)$$

$$\text{where,} \quad a = \int_0^s \kappa(s', t) ds', \quad b = \int_0^s \tau(s', t) ds' \quad \text{and} \quad c = \sqrt{a^2 + b^2},$$

and  $\mathbf{C}(t)$  is a pure time-dependent matrix in general. As by definition the first row of the matrix  $\mathbf{W}$  represents the components of the tangent, the identification  $dx_i/ds = W_{1i}(s, t)$  immediately leads to the space coordinates of the curve as,

$$x^i(s, t) = \int_0^s W_{1i}(s', t) ds' + x_0^i(t), \quad (8)$$

subjected to arbitrary initial conditions. In terms of the elements of matrices  $\mathbf{M}$  and  $\mathbf{C}$  of Eq. 6 this expression becomes,

$$x^i(s, t) = \sum_{k=1}^3 C_{ki} \int_0^s M_{1k}(s', t) ds' + x_0^i(t), \quad (9)$$

where  $M_{1k}(s, t)$ s are given in Eq. 7.

Following the expression of coordinates of the curve in Eq. 9 in terms of  $\kappa$  and  $\tau$  through Eq. 7, we are in a position to use the Hasimoto map of Eq. 3 to express  $x_i(s, t)$  directly in terms of the amplitude  $q(s, t)$ , thereby obtaining the IHM. The corresponding expressions are:

$$\kappa(s, t) = |q(s, t)| \quad \text{and} \quad \tau(s, t) = -i \frac{d}{ds} \log \left( \frac{q(s, t)}{|q(s, t)|} \right), \quad (10)$$

and thus,

$$a = \int_0^s |\psi(s, t)| ds' \quad \text{and} \quad b = -i \log \left( \frac{\psi(s, t)}{|\psi(s, t)|} \right). \quad (11)$$

Now for a given solution  $q(s, t)$  and a judicious choice of the initial conditions through  $\mathbf{C}$ , the curve dynamics can be obtained through Eq. 9 by utilizing Eq.s 7 and 11.

## 2 The IHM for the NLS solution

As a concrete demonstration of the IHM we consider the standard NLS system of Eq. 2. As mentioned already the Hasimoto map in this case relates the spin orientation of 1-D Heisenberg XXX model in the continuum limit [19] to the solution of an NLS system. The spin orientation itself is identified as the tangent to the Frenet-Serret curve. A standard ‘bright’ soliton solution of this system has the form (here we use the parameter conventions of Ref. [8]):

$$q(s, t) = [2\rho^2 \text{sech}^2 \{\rho(s - vt - s_0)\}] \exp \left\{ i2 \left( \rho^2 t - \frac{v^2}{4} t + \frac{v}{2} s \right) \right\}, \quad (12)$$

with deformation parameter velocity  $v$  and scaling  $\rho$ . The IHM parameters can directly be constructed from the above solution as,

$$a = 2\rho \tanh \{\rho(s - vt - s_0)\} \quad \text{and} \quad b = 2 \left( \rho^2 t - \frac{v^2}{4} t + \frac{v}{2} s \right). \quad (13)$$

which are connected to the curvature and torsion of the curve respectively. The simple but judicious choice of the initial conditions [18]:

$$\mathbf{C}(t) \equiv \begin{bmatrix} 0 & 0 & 0 \\ 0 & 1 & -1 \\ 1 & 0 & 0 \end{bmatrix}, \quad (14)$$

then leads to the coordinates of the evolving space curve as,

$$x^1(s, t) - x_0^1(t) \equiv \int_0^s M_{13}(s', t) ds', \quad x^2(s, t) - x_0^2(t) \equiv \int_0^s M_{12}(s', t) ds' \equiv -x^3(s, t) + x_0^3(t), \quad (15)$$

wherein,

$$\begin{aligned}
I_{12} &:= \int_0^s M_{12}(s', t) ds' \\
&= \int_0^s \frac{\rho \tanh \{\rho(s - vt - s_0)\}}{\sqrt{\rho^2 \tanh^2 \{\rho(s - vt - s_0)\} + \left(\rho^2 t - \frac{v^2}{4} t + \frac{v}{2} s\right)^2}} \\
&\quad \times \sin \left[ 2\sqrt{\rho^2 \tanh^2 \{\rho(s - vt - s_0)\} + \left(\rho^2 t - \frac{v^2}{4} t + \frac{v}{2} s\right)^2} \right] ds \quad \text{and} \\
I_{13} &:= \int_0^s M_{13}(s', t) ds' \\
&= \int_0^s \frac{\rho \tanh \{\rho(s - vt - s_0)\} \left(\rho^2 t - \frac{v^2}{4} t + \frac{v}{2} s\right)}{\rho^2 \tanh^2 \{\rho(s - vt - s_0)\} + \left(\rho^2 t - \frac{v^2}{4} t + \frac{v}{2} s\right)^2} \\
&\quad \times \left[ 1 - \cos \left( 2\sqrt{\rho^2 \tanh^2 \{\rho(s - vt - s_0)\} + \left(\rho^2 t - \frac{v^2}{4} t + \frac{v}{2} s\right)^2} \right) \right] ds \quad (16)
\end{aligned}$$

Here we have replaced the integration variable  $s'$  by  $s$  for brevity. These integrals are hard to evaluate exactly mandating a perturbative approach (Appendix A). Up to the second order of perturbation  $I_{12}$  is plotted as a function of  $s$  and time  $t$  which can be seen in Fig. 1a. The plot shows sharp singularities that could be attributed to localization of the particular soliton in Eq. 12, an assertion which will latter appear to be more convincing. In particular, on comparing with Eq. 3, the curvature  $\kappa$  of the curve captures the amplitude of the NLS solution and therefore the localization effect. The latter causes a local change in curvature and hence a discontinuity in the Frenet-Serret coordinates  $x^i(s, t)$  from the expressions of  $I_{12}$  and  $I_{13}$ . The corresponding plot for  $I_{13}$  is depicted in Fig. 1b. It also has singularity (localization)

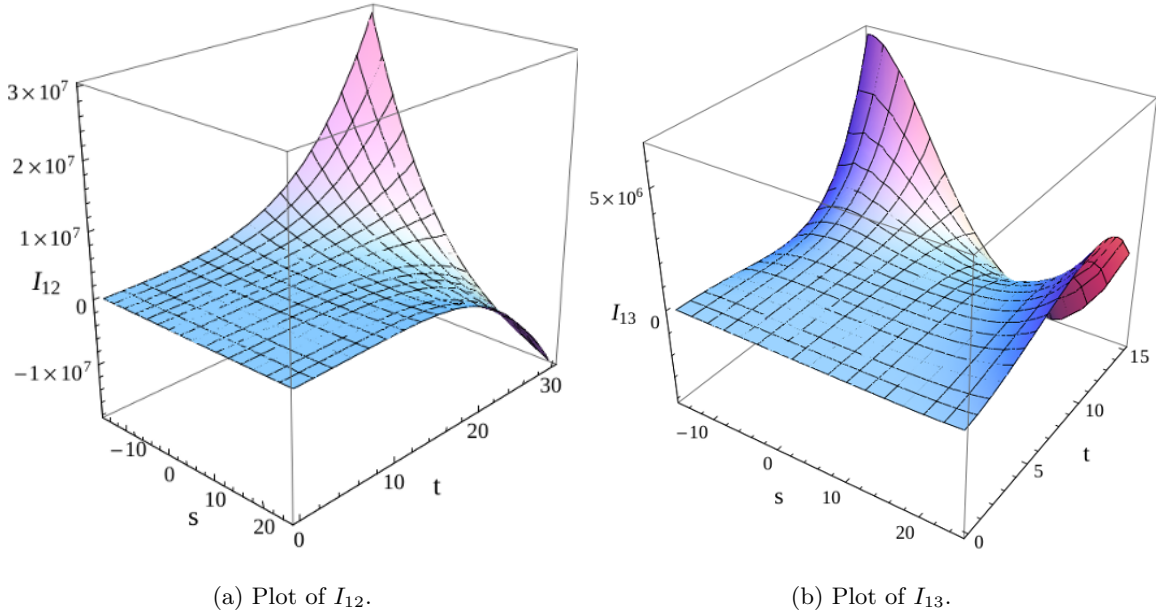
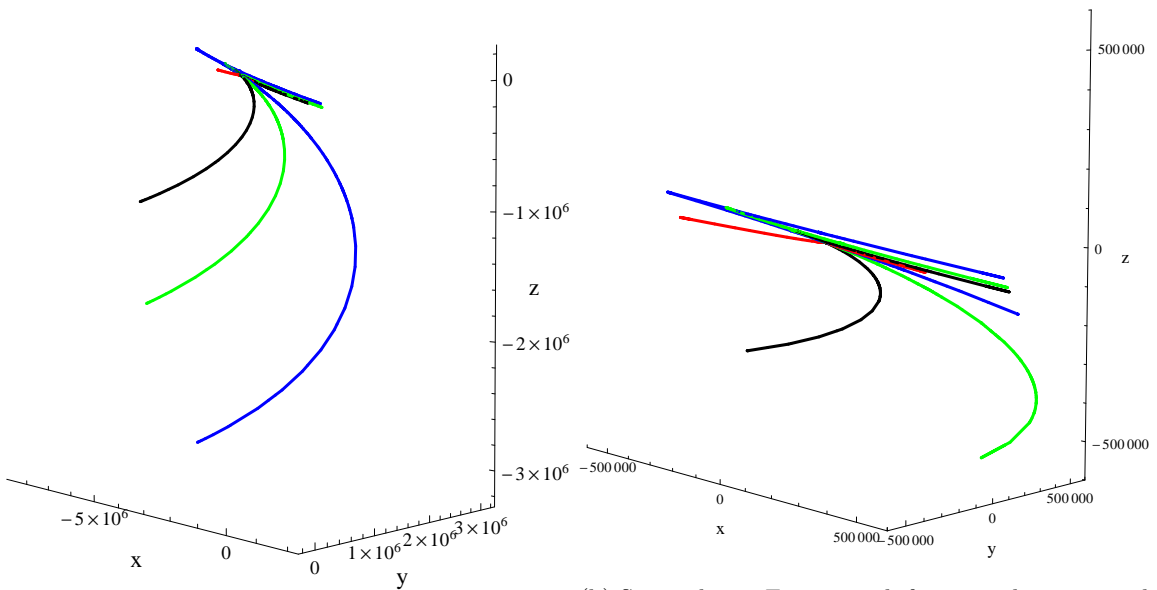


Figure 1: Plots of the integrals corresponding to the IHM  $I_{12}$  and  $I_{13}$  as a function of  $s$  (depicted as  $x$ ) and  $t$ . Here  $\rho, v = 1, s_0 = 0$  and thus  $\gamma = \frac{5}{2}t$ . Both are smooth apart from a bordering singularity corresponding to the localization of the original NLS solution.

property as expected. Therefore an expression is obtained for the space-curve coordinate  $\mathbf{x}$  as a function of both space  $s$  and time  $t$ . It so appears that the parameters  $\alpha$  and  $\beta$  always appear in the combination

$$\gamma := 2\alpha + v\beta = 2\rho^2 + \frac{1}{2}v^2t + vs_0,$$

which may be considered as the effective phase of evolution of the system. Since the integrals  $I_{12,13}$  determine the Frenet-Serret coordinates, we are now in a position to realize the combined effect that is the evolution of the curve in terms of the coordinates  $x^i(s, t)$  (with  $x_1 = x$ ,  $x_2 = y$  and  $x_3 = z$ ) which is depicted in Fig. 2a. The curve traces a *plane* in the Frenet-Serret space by pivoting about a reason containing the evolution of a singularity in the curve, the latter directly derives from the singular behavior of  $I_{12,13}$ . The evolution in the neighborhood of this pivot is explicated in Fig. 2b. This curve evolution can directly be traced back to the time dependence of the localized NLS amplitude. The plane of evolution for the Frenet-Serret curve is illustrated in Fig. 3 wherein there is a crowding near the pivotal region indicating strong overlapping (Fig. 3b).

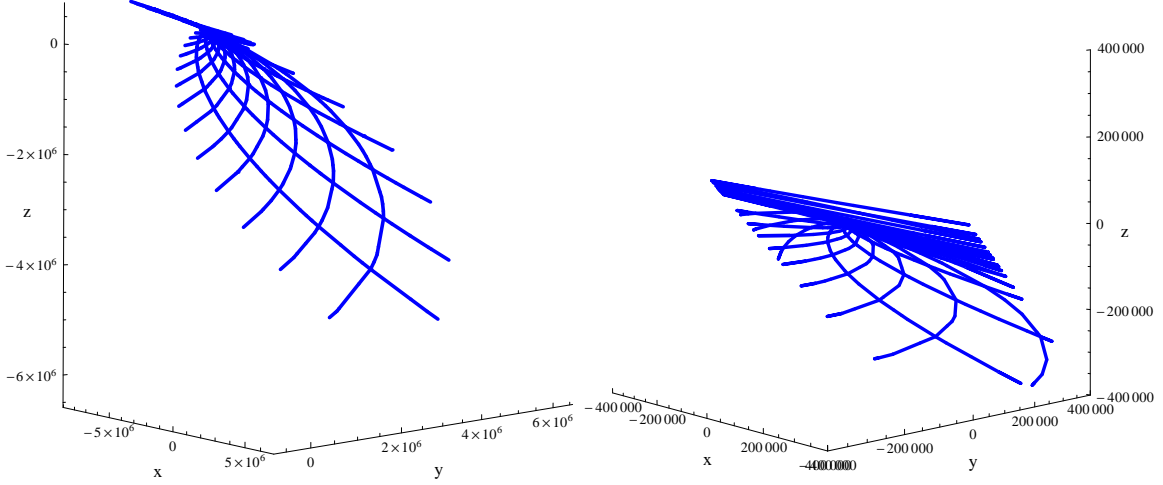


(a) The curve traces a plane with its evolution with a part. The discontinuity also evolves with time pivoted about an overlap.

Figure 2: Plots of the Frenet-Serret curve in real 3-D coordinate space  $(x,y,z)$  with parametric dependence on  $-25 \leq s \leq 25$  for different times  $t = 2$  (red), 8 (black), 10 (green), 12 (blue) with  $\rho, v = 1$   $s_0 = 0$  and thus  $\gamma = \frac{5}{2}t$  for the initial values  $x_0^{1,2,3}(t) = 0$ .

### 3 The Effect of Deformations

Deformed integrable systems are of interest as they model physical systems more accurately. Since the latter are always finite, they cannot be explained completely by a field theory with infinite degrees of freedom, *e. g.*, an integrable one. In particular QI and NH deformations of integrable systems are of special interest. QID [7, 8] renders at most a subset of charges of the undeformed system to be conserved, thereby depicts a *deviation* from complete integrability. Such a model depicts a physical system more correctly. On the other hand NHD [9, 10] *maintains* integrability but at a cost of additional constraints in the solution space. This allows for constructing many new hierarchies from a known system, which is very likely to reflect various real systems, with related dynamical properties.



(a) Evolution of *one* undeformed curve on a surface (b) The ‘crowding’ formed by overlapping evolution of which turns out to be flat. the singular part of the curve signifying localization.

Figure 3: Surface traced by the undeformed curve.

In the following we study the effect of such deformations on the IHM of the NLS system. More specifically we focus on the effect of these deformations on the solitonic sector and the corresponding distinct signatures on curve evolution in the Frenet-Serret space. Such an analysis should reveal aspects of integrability and constrained nonlinear dynamics in a more graphical way.

### 3.1 Effect of QI Deformation

The QI deformation of the NLS system deviates the original system from complete integrability. This can be quantified in terms of a small parameter  $\varepsilon \rightarrow 0$  that distorts the corresponding soliton solution in Eq. 12 to [8]:

$$\psi(s, t) = [(2 + \varepsilon)\rho^2 \operatorname{sech}^2 \{(1 + \varepsilon)\rho(s - vt - s_0)\}]^{1/(1+\varepsilon)} \exp \left\{ i2 \left( \rho^2 t - \frac{v^2}{4} t + \frac{v}{2} s \right) \right\}, \quad (17)$$

Such distortion effects the modulus parameter  $a$  only of IHM and leaves the ‘phase’ parameter  $b$  alone. As is customary [8], we expand up to the *first order* in  $\varepsilon$  (The higher order contributions are tediously long and some of them cannot be evaluated in a closed form. We neglect them as they are obviously sub-dominant.) as,

$$|\psi(s, t)| = [(2 + \varepsilon)\rho^2 \operatorname{sech}^2 \{(1 + \varepsilon)\rho(s - vt - s_0)\}]^{1/(1+\varepsilon)} \\ \approx 2\rho^2 \operatorname{sech}^2(x) + \varepsilon\rho^2 [\operatorname{sech}^2(x) \{1 - 2 \log(2\rho^2 \operatorname{sech}^2(x))\} - 4x \tanh(x) \operatorname{sech}(x)]. \quad (18)$$

The IHM parameter  $a$  thus can be approximated as:

$$a(s, t) \approx 2\rho \tanh(x) + \varepsilon\rho [5 \tanh(x) + 4 \operatorname{sech}(x) - 2 \tanh(x) \log \{2\rho^2 \operatorname{sech}^2(x)\} - 4x]. \quad (19)$$

The  $\varepsilon$ -dependent correction integrals  $I_{12,13}(\varepsilon)$  for the QID case are obtained in Appendix B which are plotted in Fig.s 4a and 4b respectively. They are seen to be well-behaved (no singularity) within the

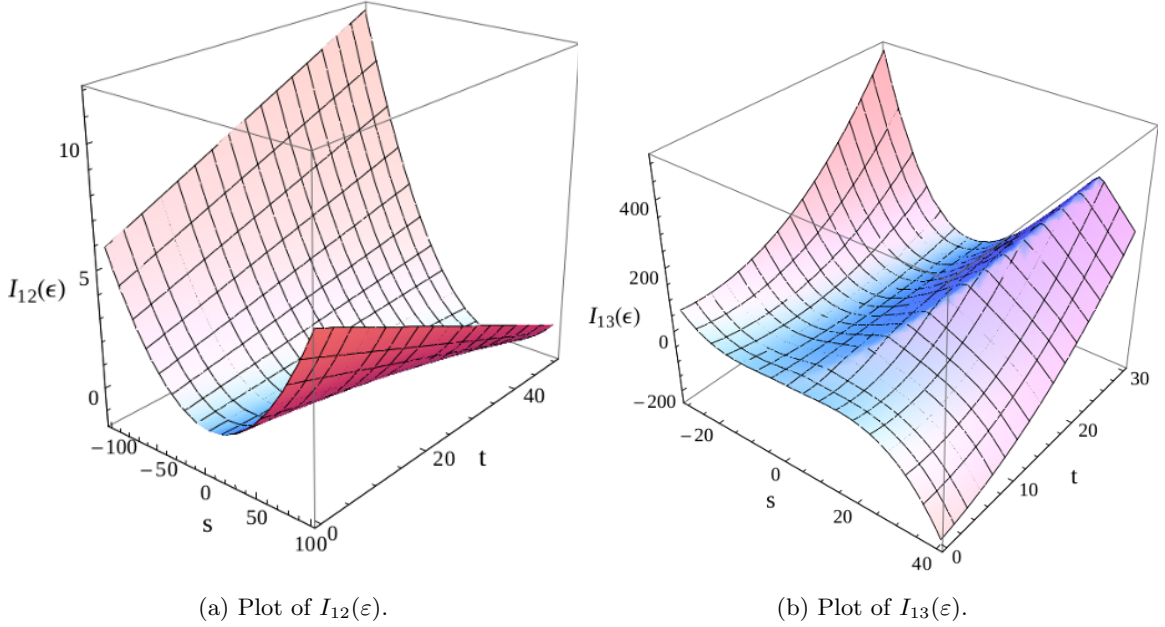


Figure 4: Plots of  $\epsilon$ -dependent parts of the quasi-deformed integrals  $I_{12}$  and  $I_{13}$  as a function of  $s$  and  $t$ . Herein  $\rho, v = 1, s_0 = 0; \epsilon = 0.01$  and thus  $\gamma = \frac{5}{2}t$ . They almost behave similarly to the undeformed counterparts of Fig. 1.

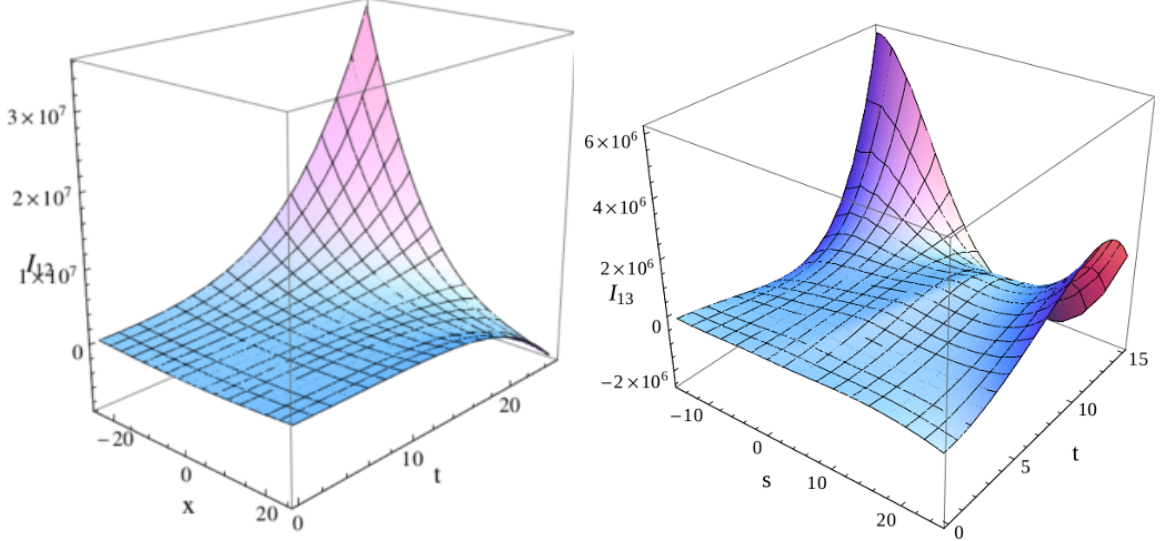
domains of validation corresponding to undeformed integrals  $I_{12}$  and  $I_{13}$  (Fig. 1) and are much smaller in magnitude, thereby validating our scheme of approximation. This is further supported by the plots of the complete integrals  $I_{12,13}$  including the quasi-deformations in Figs. 5a and 5b which only slightly differ from their undeformed counterparts. However, the perturbative difference is a local maximum (Figs. 4b and 5b) which should signify deformation in the analytic structure of the corresponding dynamical solution (the NLS soliton) owing to deviation from exact integrability.

The distinct feature of QID is most clearly demonstrated by the evolution of the ‘quasi-deformed’ Frenet-Serret curve. The corresponding plots are depicted in Fig. 6. Though the curve still evolves on a plane similar to the undeformed case (Fig. 2) the evolution is clearly different near the pivotal regions (Figs. 2b and 6b). The perturbative ( $\epsilon$ -dependent) modifications become significant near the singularity of the curve, thereby removing its overlap under evolution (or dispersing the pivotal structure). This overlap was a signature of solitonic integrability in the undeformed case. This essentially supports the ongoing scheme of approximation. Finally, the plane of evolution of the quasi-deformed Frenet-Serret curve is depicted in Fig. 7. Although the orientation remains the same, the deformed plane has a modified shape of curve evolution. This is expected since the  $\epsilon$ -deformation is subjected to the original parameterization of the undeformed system. Since a quasi-integrable system is supposed to *asymptotically coincide* with its integrable counterpart [7, 8], any characteristic of deformation must be limited to the localized behavior. This is clearly highlighted by the erratic evolution near the pivotal region (Fig. 7b) marking singularity dispersion.

### 3.2 Effect of Non-holonomic Deformation

The formal introduction of NHD to the NLS system can be made through a generalized NLS Lax pair of the form:

$$\begin{aligned}
 A &= -i\lambda\sigma_3 + \kappa^* q^* \sigma_+ + \kappa q \sigma_- \quad \text{and} \\
 B &= i(2\lambda^2 - \eta|q|^2)\sigma_3 - (2\lambda\kappa^* q^* + i\kappa^* q_s^*)\sigma_+ - (2\lambda\kappa q - i\kappa q_s)\sigma_-,
 \end{aligned} \tag{20}$$



(a) Plot of  $I_{12}(\varepsilon = 0) + I_{12}(\varepsilon)$  with  $\varepsilon = 145.9$ .

(b) Plot of  $I_{13}(\varepsilon = 0) + I_{13}(\varepsilon)$  with  $\varepsilon = 146$ .

Figure 5: The complete plots of quasi-deformed integrals  $I_{12}$  and  $I_{13}$  as a function of  $s$  and  $t$ . Herein  $\rho, v = 1, s_0 = 0$  and thus  $\gamma = \frac{5}{2}t$ . We have considered much higher values of  $\varepsilon$  ( $\sim 100$ ) than those earlier in Figs 4a and 4a ( $\sim 0.01$ ) so that quasi-distortions are resolvable, yet perturbative. Comparing with Figs 1a and 1b the said deformation effects sub-dominant as expected. More importantly, they complement the undeformed structures.

in the  $sl(2)$  representation:  $[\sigma_3, \sigma_{\pm}] = \pm 2\sigma_{\pm}$ ,  $[\sigma_+, \sigma_-] = \sigma_3$ . Herein, the coefficients are local to begin with:  $\eta = \eta(s, t)$  and  $\kappa = \kappa(s, t)$  and  $\lambda$  is the spectral parameter. The usual NLS system  $iq_t + q_{ss} - 2q|q|^2 = 0$  is obtained from the zero curvature condition (ZCC):

$$F_{ts} = A_t - B_s + [A, B] = 0,$$

that imposes the condition  $\eta = -|\kappa|^2$  for consistency. However, it further restricts these coefficients to be independent of space. This prohibition to inhomogeneity by the integrability structure can be lifted through suitable NHD. It makes sense as NHD induces modified time-evolution that allows for compensating space evolution maintaining integrability and preserving the scattering data. It is obtained by perturbing the temporal Lax component as:

$$\delta B = \frac{i}{2} (f_i + \lambda^{-1} h_i) \sigma_i, \quad i = 3, \pm. \quad (21)$$

where  $f_{is}$  and  $h_{is}$  are local parameters. Then the ZCC yields the dynamical equation:

$$\kappa (q_t - iq_{ss} - 2i\eta|q|^2 q) - i\kappa_s q_s + \kappa_t q - \frac{i}{2} (f_{-,s} - 2\kappa q f_3) = h_-, \quad (22)$$

where  $h_-^* = -h_+$  and  $f_-^* = f_+$ , accompanied by the conditions:

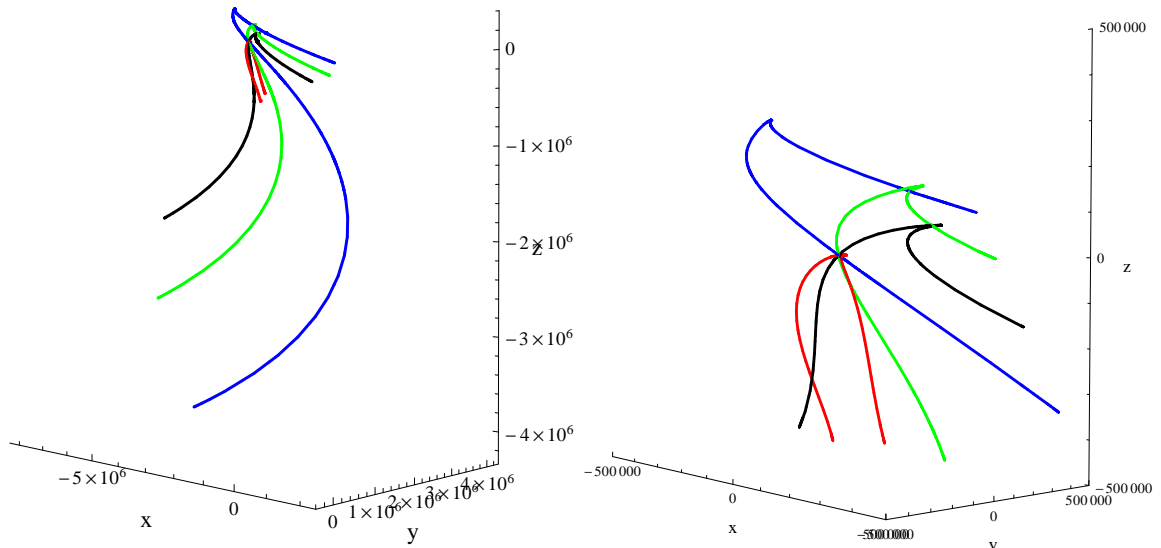
$$(\eta|q|^2)_s + |\kappa|^2 |q|_s^2 - \frac{1}{2} (f_{3,s} + \kappa q f_+ - \kappa^* q^* f_-) = 0 \quad \text{and} \quad \kappa_s q - \frac{1}{2} f_- = 0, \quad (23)$$

that ensure locality of the original coefficients. The coefficients  $h_{is}$  constraint the dynamical variable at higher order of derivatives:

$$h_{3,ss} = 4|p|^2 h_3 - 2\text{Re}(p_s h_+), \quad p = \kappa q, \quad (24)$$

which is the characteristic of NHD [10], restricting only the solution-space but *not* the dynamics. The above conditions of the deformation parameters allows for the dynamical equation to take the form:





(a) The quasi-deformed curve, although different in shape, also traces a plane like the undeformed one in Fig. 2a. They still group near the discontinuity. (b) Focusing on the non-trivial part of Fig. 6a, the singularities are found to be deformed and more resolved than that in the undeformed case (Fig. 2b).

Figure 6: The 3-D coordinate space  $(x,y,z)$  evolution of the quasi-deformed curve with parametric dependence on  $-25 \leq s \leq 25$  for different times  $t = 2$  (red), 8 (black), 10 (green), 12 (blue) with  $\rho, v = 1, s_0 = 0$  and thus  $\gamma = \frac{5}{2}t$  for the initial values  $x_0^{1,2,3}(t) = 0$  and  $\varepsilon = 146$ . Though the effect of the quasi-deformation is clear it essentially follow the pattern of the original dynamics and effectively resolves the grouping of singularities.

$$ip_t + p_{ss} - 2p|p|^2 = ih_-, \quad (25)$$

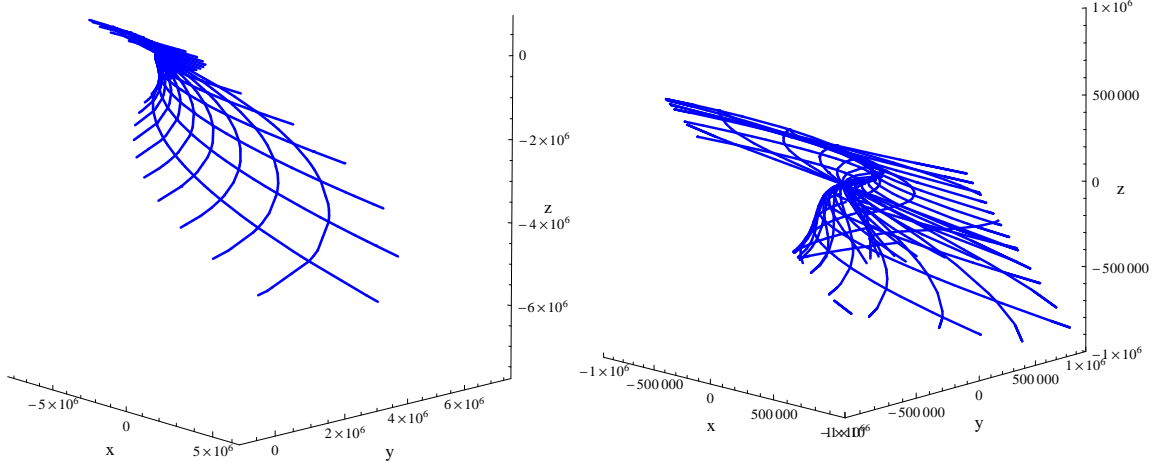
which is just the scaled NLS system for the locally scaled variable  $p(s,t) = \rho(s,t)q(s,t)$  having a source  $ih_-$ . Eq. 21 provides the most general NHD possible for the NLS system within its characteristic spectral domain. Even a simpler case with  $h_i = 0$  allows for the same local scaling of Eq. 25 but without the source. Interestingly the coupling is also scaled to unity as the old (local) coupling is absorbed by the scaling to  $p$ . Also, the exact equation satisfied by the now-local variable  $\rho(s,t)$  mirrors that of  $q(s,t)$  underlying a *duality* of this general system.

The generality of this deformation prompts us to interpret any particular NHD of the NLS system as a local scaling of the undeformed solution. A comparison between the space curve dynamics of the deformed and undeformed case could shade more light on the observed local scaling due to the NHD. To obtain the IHM of the non-holonomic NLS system we consider the following known soliton solution of Ref. [20]:

$$q = 2\rho_d^2 \text{sech}^2 \left[ \rho_d (s - v_d t - x_0) \right] \exp \left[ i2 \left( \rho_d^2 t - \frac{v_d^2}{4} t + \frac{v_d}{2} s \right) \right], \quad (26)$$

which resembles the undeformed counterpart apart from the modified dynamical parameters. The modified velocity  $v_d = v + v'$  has the non-holonomic perturbation  $v' = \tilde{c}(t)/t|\lambda_1|^2$  and the modified frequency  $\rho_d v_d = \rho v + \omega'$  contains the corresponding extension  $\omega' = -2\rho(x - vt)\tilde{c}(t)/t|\lambda_1|^2$ . Here  $\lambda_1 = \rho(x - vt) + i\eta$  with  $\eta$  being a deformation parameter and  $\tilde{c}(t)$  corresponds to the asymptotic value of the perturbing function. For  $|x| \rightarrow \infty$  these perturbed parameters regain the undeformed values.

The fact that NHD exclusively modifies the temporal Lax component thereby allotting time dependence to dynamic parameters *in general*. However, the zero curvature condition still prevails through additional constraints ordered higher than the dynamical equation itself, thereby maintaining integrability. Of



(a) The  $\varepsilon$ -deformed evolution of the curve still traces a plane in the 3-D space as in Fig. 3b although the erratic behavior in comparison to the undeformed shape is different. (b) A closer inspection of the singular region unveils a plane in the 3-D space as in Fig. 3b although the erratic behavior in comparison to the undeformed case.

Figure 7: Surface traced by the quasi-deformed curve.

particular interest are the deformed systems whose dynamics do not develop explicit time-dependence, technically known as *semi-holonomic* [21]. The time dependence of the non-holonomic deformation parameters  $v' \sim t\rho^{-2}(s-vt)^{-2}$  and  $\omega' \sim t\rho^{-1}(s-vt)^{-1}$  can conform to this property. The analysis could be subjected to large enough values of  $s-vt$ , especially as we are dealing with localized systems, so that these parameters are perturbative and smaller still than the parameter  $\theta$  in Eq. 30 of Appendix A. This is essential to obtain a sensible expansion *without* contradicting the previous (undeformed) ones. It readily follows that,

$$\rho_d = \rho + \rho', \quad \rho' \approx \frac{1}{v}(\omega' - \rho v') \ll \rho. \quad (27)$$

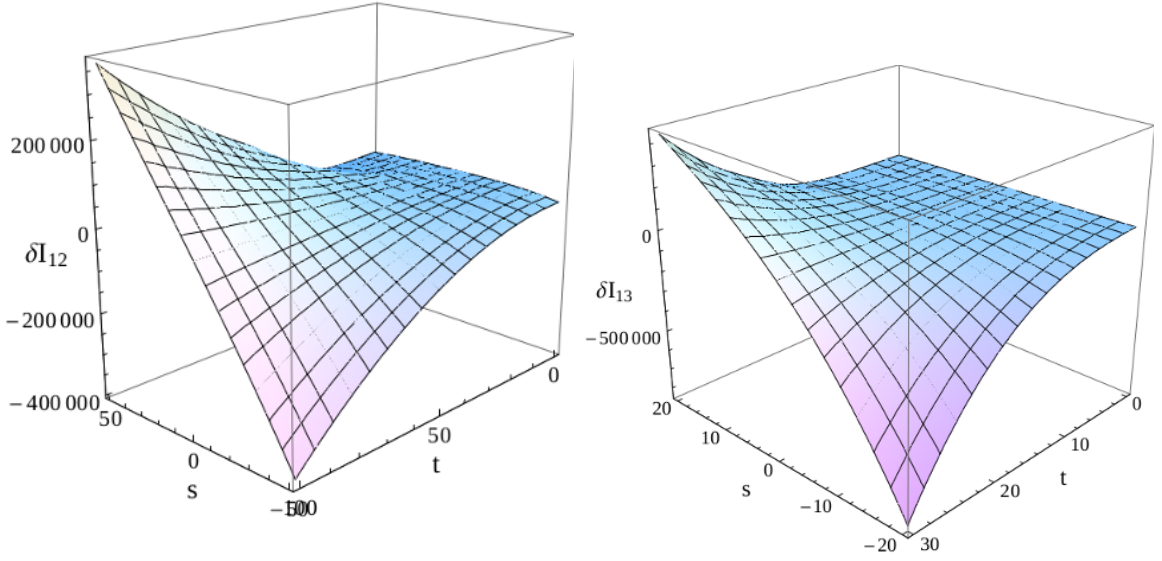
On considering the ‘primed’ variables to be even smaller, an approximate expansion leads to:

$$q \approx 2\rho^2 \operatorname{sech}^2 \{\rho(s-\beta)\} \exp \{i(2\alpha + vs)\} \left[ 1 - 2 \{ \rho'(s-\beta) - \rho v't \} \tanh \{ \rho(s-\beta) \} + 2 \frac{\rho'}{\rho} + i(4\rho\rho't - vv't + v's) \right]. \quad (28)$$

This indeed is a *local scaling* of the undeformed solution (Eq. 12) in the same sense as in Eq. 25. Though it is an approximate expression the presence of the higher order constraint condition(s) (Eq. 24) severely restricts the allowed solution space spanned by  $p = \kappa q$  which should restrict the values of the deformation parameters  $\rho'$  and  $v'$  to perturbative ones, a point that is further valid from a physical point-of-view. The Fenet-Serret parameters can be read off immediately as,

$$\begin{aligned}
\kappa &= |q| \approx 2\rho^2 \operatorname{sech}^2 \{\rho(s - \beta)\} \\
&\quad \times \sqrt{\left\{1 + 2\frac{\rho'}{\rho} - 2\{\rho'(s - \beta) - \rho v't\} \tanh \{\rho(s - \beta)\}\right\}^2 + (4\rho\rho't - vv't + v's)^2}, \\
\tau &\approx -i \frac{d}{dx} \log \left[ \frac{1 + 2\frac{\rho'}{\rho} - 2\{\rho'(s - \beta) - \rho v't\} \tanh \{\rho(s - \beta)\} + i(4\rho\rho't - vv't + v's)}{\sqrt{\left\{1 + 2\frac{\rho'}{\rho} - 2\{\rho'(s - \beta) - \rho v't\} \tanh \{\rho(s - \beta)\}\right\}^2 + (4\rho\rho't - vv't + v's)^2}} \right. \\
&\quad \left. \times \exp \{i(2\alpha + vs)\} \right]. \quad (29)
\end{aligned}$$

The effect the above modifications to the integrals  $I_{12}$  and  $I_{13}$  are evaluated in Appendix C and the corresponding plots are depicted in Figs 8a and 8b respectively. These contributions are well-behaved and are free from any local maximum, unlike the QID counterparts, as expected. They behave simply as sub-dominant extensions to the undeformed counterparts of Fig. 1 as confirmed by the plots including the NHD contributions in Fig. 9.

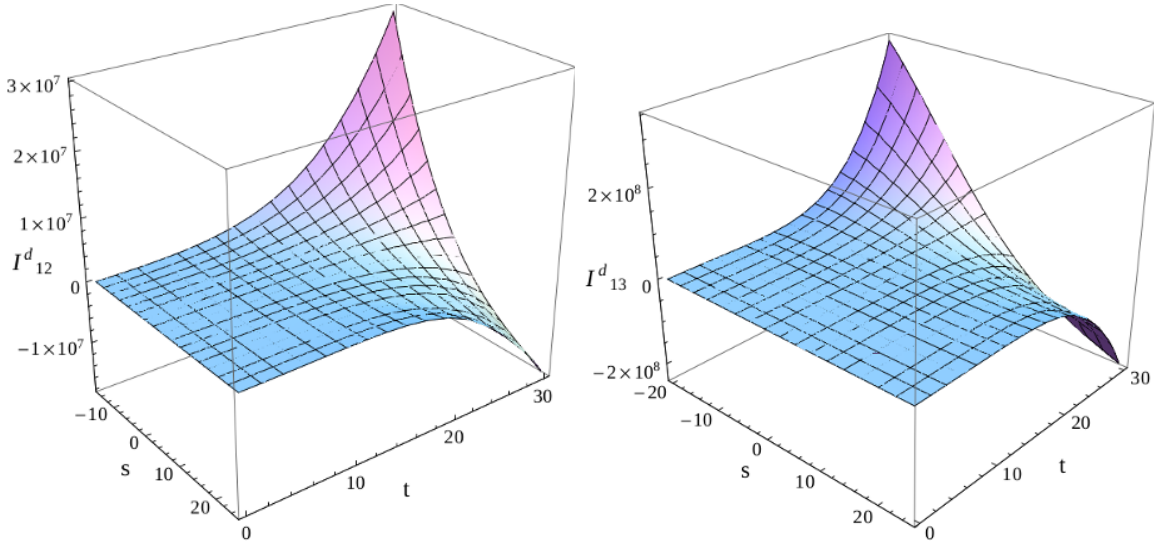


(a) Plot of the non-holonomically deformed contribution  $\delta I_{12} = I_{12}^d - I_{12}$ .

(b) Plot of the non-holonomically deformed contribution  $\delta I_{13} = I_{13}^d - I_{13}$ .

Figure 8: Plots of contributions due to NHD to the integrals  $I_{12}$  and  $I_{13}$  as functions of  $s$  and  $t$ . Here the carried-over original values  $\rho v = 1$ ,  $s_0 = 0$  (so  $\gamma = \frac{5}{2}t$ ) are complemented by the NHD parameters fixed as  $\rho', v' = 0.1$ . Their regular behaviour conforms to the undeformed counterparts in Figs 1a and 1b as NHD is integrability-preserving.

It can be observed that the effect of NHD is prominent mostly away from the region where the dynamical solution is localized (in terms of coordinate  $s$ ). This was not the case for QID as a local ‘hump’ appeared (Fig 4b). This may be considered as an effective quantitative difference between QID and NHD that is directly concerned with the fact that whether integrability is preserved or not. The evolution of the corresponding Frenet-Serret curve in the space in Fig. 10 agrees with this conclusion. The curve remains almost unchanged from the undeformed case (Fig. 2) which re-iterates the scaling nature of the NHD. At most, there is an overall local scaling which uniformly modifies the curvature  $\kappa(s, t)$ . In this perturbative picture,



(a) Plot of the complete non-holonomically deformed  $I_{12}^d$ . (b) Plot of the complete non-holonomically deformed  $I_{13}^d$ .

Figure 9: Plots of the integrals  $I_{12}$  and  $I_{13}$  including the NHD contributions as functions of  $s$  and  $t$  with  $\rho v = 1$ ,  $s_0 = 0$  and  $\rho' v' = 0.1$ . The overall shapes are essentially the same as those in Figs. 1a and 1b as NHD preserves integrability with modifications at the marginal zone (9b), unlike the QID case in Fig. 5b with a very local hump.

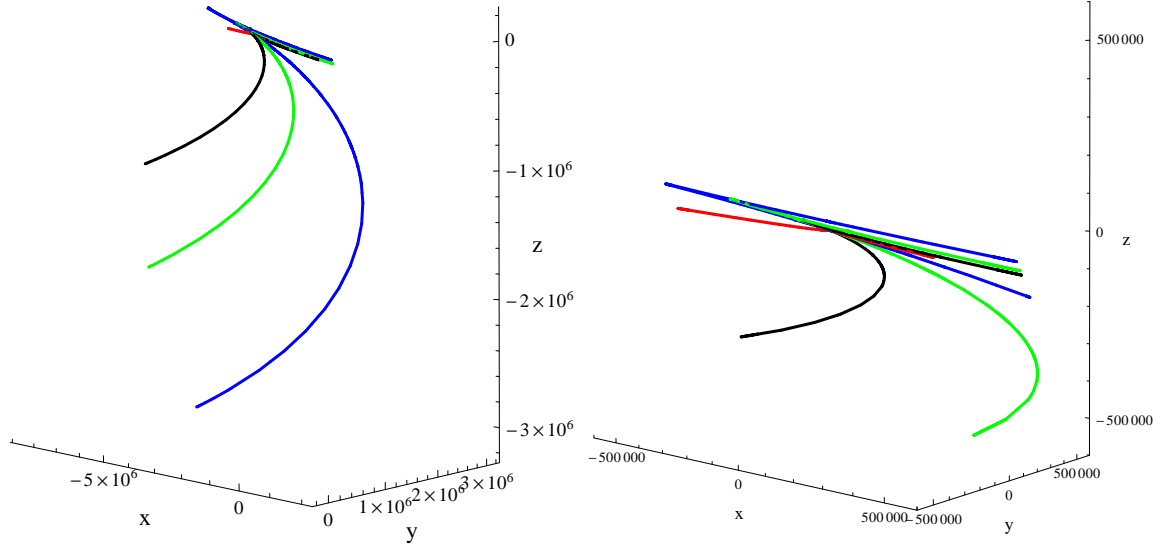
however, this effect is not directly visible. The traced plane and the pivoting singularity evolution (Fig. 11) are also almost identical to the undeformed case. On the other hand, the QID deviates from integrability and as a result the very local behavior of the curve evolution changes, namely the successive singularity overlap in the Frenet-Serret curve gets ‘resolved’ (Fig. 6b). Therefore the effect on this singularity overlap, which characterizes a localized dynamical solution, is not only the marker for deformation but also for its *kind*.

## 4 Conclusions and Discussions

We studied the in-extensible flows of curves in  $\mathbb{R}^3$  using the inverse Hasimoto transformation that corresponded to solitonic solution sector of the NLS system. The plots generated by this in-extensible curve depicted a planar evolution in  $\mathbb{R}^3$  pivoted around the evolution of the singular point that corresponds to the localized nature of the corresponding NLS soliton. This geometry of the curve is seen to be maintained under NHD as integrability is preserved whereas upon QID the deviation from integrability is marked by a ‘resolution’ of the said singular region as it also evolves. This implies very strongly that the IHM can be a direct geometrical demonstration of integrability (or loss of it) in localized dynamical systems.

It would be worthwhile to expand the IHM approach to other localized sectors of the NLS system, such as multi-soliton solutions, and to systems which are related to the the NLS system dynamically. One particular type of system of interest would be the non-local NLS equation that supports localized dynamics [22]. Since the localization is a key aspect of the evolution structure of the parametric curve in  $\mathbb{R}^3$ , the manifestation of non-locality thereon will be interesting. Further, this may help in understanding the dynamics of the non-local solutions, which are of vibrant interest currently, in better light.

**Acknowledgement:** The authors are thankful to Dr. Indranil Mukherjee for many discussions and valuable comments. KA’s work was done at and supported by the IF, Naresuan University, Thailand.



(a) The non-holonomically deformed curve continues to trace a plane like the undeformed counterparts. They also group near the discontinuity. (b) Focusing the non-trivial part of Fig. 10a, the singularities remain unresolved unlike that in the QID case (Fig. 6b) almost exactly same as Fig. 2b.

Figure 10: The 3-D curve evolution corresponding to the non-holonomically deformed solution with parametric dependence on  $-25 \leq s \leq 25$  for different times  $t = 2$  (red), 8 (black), 10 (green), 12 (blue) with  $\rho, v = 1, s_0 = 0$  and thus  $\gamma = \frac{5}{2}t$  for the initial values  $x_0^{1,2,3}(t) = 0$  and  $\rho', v' = 0.01$ . The behavior is exactly similar to that of the undeformed case, though a perturbed result, and the local singularity structure depicting a localized solution is preserved.

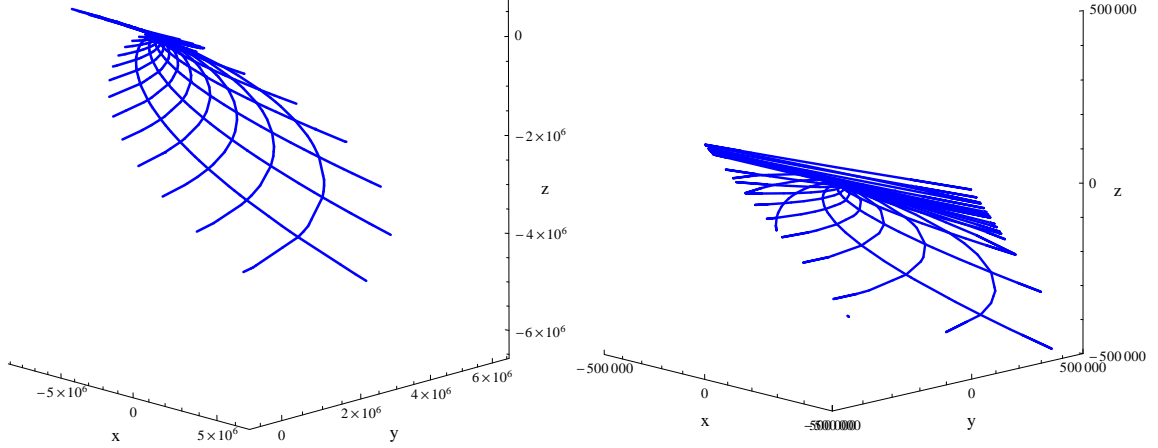
## A Integrals for Undeformed NLS Case

Since it is difficult to obtain a closed-form exact expression for the integrals in Eq.s 16 it is viable to adopt the approximation:

$$\theta = \sqrt{\rho^2 \tanh^2 \{\rho(s - vt - s_0)\} + \left(\rho^2 t - \frac{v^2}{4}t + \frac{v}{2}s\right)^2} \sim 0. \quad (30)$$

This makes sense as we can always confine to a sector with small parameters  $\rho$  and  $v$ . Then the first integral in Eq. 16 can be expanded as:

$$I_{12} \approx 2 \int_{-\rho(vt+s_0)}^X \left(1 - \frac{2}{3}\theta^2 + \frac{2}{15}\theta^4 + \dots\right) \tanh(x) dx, \quad (31)$$



(a) The non-holonomically deformed curve still traces a plane in the 3-D space as in Fig.s 3b (and 7a) and the undeformed case. (b) The behavior of the singular region complements maintains the over-all shape of the undeformed case.

Figure 11: Surface traced by the non-holonomically deformed curve.

where  $x = \rho(s - vt - s_0)$ . After evaluating the integrals corresponding to the individual powers of  $\theta$ , the results can be summed-up as,

$$\begin{aligned}
I_{12} \equiv & \left[ \frac{1}{60}(2\alpha + v\beta)^4 - \frac{1}{3}(2\alpha + v\beta)^2 + 2 \right] \int \tanh(x) + \frac{v}{3\rho}(2\alpha + v\beta) \left[ \frac{1}{5}(2\alpha + v\beta)^2 - 2v \right] \\
& \times \int x \tanh(x) + \frac{v^2}{\rho^2} \left[ \frac{1}{10}(2\alpha + v\beta)^2 - \frac{1}{3} \right] \int x^2 \tanh(x) + \frac{1}{15} \frac{v^3}{\rho^3} (2\alpha + v\beta) \\
& \times \int x^3 \tanh(x) + \frac{1}{60} \frac{v^4}{\rho^4} \int x^4 \tanh(x) \\
& + \frac{\rho^2}{3} \left[ \frac{2}{5}(2\alpha + v\beta)^2 - 4 \right] \int \tanh^3(x) + \frac{4}{15} v\rho(2\alpha + v\beta) \int x \tanh^3(x) + \frac{2}{15} v^2 \int x^2 \tanh^3(x) \\
& + \frac{4}{15} \int \tanh^5(x), \tag{32}
\end{aligned}$$

wherein,

$$\alpha := \left( \rho^2 - \frac{v^2}{4} \right) t, \quad \beta = vt + s_0 \quad \text{and} \quad \int = \int_{-\rho\beta}^x dx, \tag{33}$$

and,

$$\begin{aligned}
\int \tanh(x) &= \log [\cosh(x)] + \text{Const.}, \\
\int x \tanh(x) &= \frac{1}{2} [x \{x + 2 \log (1 + e^{-2x})\} - \text{Li}_2 (-e^{-2x})] + \text{Const.}, \\
\int x^2 \tanh(x) &= -x \text{Li}_2 (-e^{-2x}) - \frac{1}{2} \text{Li}_3 (-e^{-2x}) + \frac{1}{2} x^2 \{x + 3 \log (1 + e^{-2x})\} + \text{Const.}, \\
\int x^3 \tanh(x) &= \frac{1}{4} [-6x^2 \text{Li}_2 (-e^{-2x}) - 6x \text{Li}_3 (-e^{-2x}) - 3 \text{Li}_4 (-e^{-2x}) + x^4 + 4x^3 \log (1 + e^{-2x})] + \text{Const.}, \\
\int x^4 \tanh(x) &= -2x^3 \text{Li}_2 (-e^{-2x}) - 3x^2 \text{Li}_3 (-e^{-2x}) - 3x \text{Li}_4 (-e^{-2x}) - \frac{3}{2} \text{Li}_5 (-e^{-2x}) + \frac{1}{5} x^5 \\
&\quad + x^4 \log (1 + e^{-2x}) + \text{Const.}, \\
\int \tanh^3(x) &= \frac{1}{2} \text{sech}^2(x) + \log [\cosh(x)] + \text{Const.}, \\
\int x \tanh^3(x) &= \frac{1}{2} [-\text{Li}_2 (-e^{-2x}) + x^2 + 2x \log (1 + e^{-2x}) - \tanh(x) + x \text{sech}^2(x)] + \text{Const.}, \\
\int x^2 \tanh^3(x) &= -x \text{Li}_2 (-e^{-2x}) - \frac{1}{2} \text{Li}_3 (-e^{-2x}) + \frac{1}{3} x^3 + x^2 \log (1 + e^{-2x}) + \frac{1}{2} x^2 \text{sech}^2(x) \\
&\quad - x \tanh(x) + \log [\cosh(x)] + \text{Const.}, \\
\int \tanh^5(x) &= -\frac{1}{4} \text{sech}^4(x) + \text{sech}^2(x) + \log [\cosh(x)] + \text{Const.}, \tag{34}
\end{aligned}$$

where  $\text{Li}_n(x)$  is the  $n$ -th order poly-logarithmic function. These integrals are to be evaluated within the limits  $X$  and  $-\rho\beta$ .

In a similar fashion, the second integral in Eq.s 16,

$$I_{13} \approx \int_{-\rho\beta}^X \left( \alpha + \frac{v}{2}s \right) \left( 2 - \frac{2}{3}\theta^2 + \frac{4}{45}\theta^4 + \dots \right) \tanh(x) dx, \tag{35}$$

again upto  $\mathcal{O}(\theta^4)$ , takes the form:

$$\begin{aligned}
I_{13} &\approx \frac{2}{45} v \rho^3 \int x \tanh^5(x) dx + \frac{2}{45} (2\alpha + v\beta) \rho^4 \int \tanh^5(x) dx + \frac{1}{45} \frac{v^3}{\rho} \int x^3 \tanh^3(x) dx \\
&\quad + \frac{3}{45} v^2 (2\alpha + v\beta) \int x^2 \tanh^3(x) dx + \left[ \frac{1}{9} \rho v (2\alpha + v\beta)^2 - \frac{1}{3} \rho v \right] \int x \tanh^3(x) dx \\
&\quad + \left[ \frac{2}{45} \rho^2 (2\alpha + v\beta)^3 - \frac{1}{3} \rho^2 (2\alpha + v\beta) \right] \int \tanh^3(x) dx \\
&\quad + \frac{1}{360} \frac{v^5}{\rho^5} \int x^5 \tanh(x) dx + \frac{1}{60} \frac{v^4}{\rho^4} (2\alpha + v\beta) \int x^4 \tanh(x) dx + \frac{1}{6} \left[ \frac{1}{6} \frac{v^2}{\rho^2} (2\alpha + v\beta)^2 - \frac{v^3}{\rho^3} \right] \\
&\quad \times \int x^3 \tanh(x) dx + \frac{1}{3} \frac{v^2}{\rho^2} (2\alpha + v\beta) \left[ \frac{1}{12} (2\alpha + v\beta)^2 - 1 \right] \int x^2 \tanh(x) dx + \frac{v}{\rho} \left[ \frac{1}{72} (2\alpha + v\beta)^4 \right. \\
&\quad \left. - \frac{1}{4} (2\alpha + v\beta)^2 + 1 \right] \int x \tanh(x) dx + (2\alpha + v\beta) \left[ \frac{1}{360} (2\alpha + v\beta)^4 - \frac{1}{12} (2\alpha + v\beta)^2 + 1 \right] \\
&\quad \times \int \tanh(x) dx, \tag{36}
\end{aligned}$$

pertaining to the integrals in Eq.s 34 and,

$$\begin{aligned}
\int x^5 \tanh(x) &= \frac{1}{12} \left[ -30x^4 \text{Li}_2(-e^{-2x}) - 60x^3 \text{Li}_3(-e^{-2x}) - 90x^2 \text{Li}_4(-e^{-2x}) - 90x \text{Li}_5(-e^{-2x}) \right. \\
&\quad \left. -45 \text{Li}_6(-e^{-2x}) + 2x^6 + 12x^5 \log(1 + e^{-2x}) \right] + \text{Const.}, \\
\int x^3 \tanh^3(x) &= \frac{1}{4} \left[ -6(1+x^2) \text{Li}_2(-e^{-2x}) - 6x \text{Li}_3(-e^{-2x}) - 3 \text{Li}_4(-e^{-2x}) + (4x^3 + 12x) \log(1 + e^{-2x}) \right. \\
&\quad \left. + x^4 + 2x^3 \text{sech}^2(x) + 6x^2 - 6x^2 \tanh(x) \right] + \text{Const.}, \\
\int x \tanh^5(x) &= \frac{1}{12} \left[ -6 \text{Li}_2(-e^{-2x}) + 6x \{x + 2 \log(1 + e^{-2x})\} - 10 \tanh(x) - 3x \text{sech}^4(x) \right. \\
&\quad \left. + \{12x + \tanh(x)\} \text{sech}^2(x) \right] + \text{Const.} \tag{37}
\end{aligned}$$

## B Integrals for Quasi-deformed NLS Case

Following the analysis for the undeformed case (Appendix A), it is beneficial to obtain the deviations caused to different powers of the undeformed perturbation parameter (Eq. 30) as:

$$\begin{aligned}
\theta^2(\varepsilon) &\approx \theta^2(\varepsilon = 0) + \varepsilon \rho \tanh(x) \quad \text{and} \\
\theta^4(\varepsilon) &\approx \theta^4(\varepsilon = 0) + 2\varepsilon \rho \tanh(x) \theta^2(\varepsilon = 0). \tag{38}
\end{aligned}$$

This further allows for the assumption that the undeformed  $\theta^2(\varepsilon = 0)$  is still small and we neglect any  $\varepsilon$ -dependent term with  $\theta^2$  (namely, the second term on the RHS of the second equation above). Therefore the quasi-modified extension to the two IHM integrals can be approximated as,

$$\begin{aligned}
I_{12}(\varepsilon) &\approx I_{12}(\varepsilon = 0) + \varepsilon \int dx \left[ -\frac{4}{3} \rho \tanh^2(x) + 5 \tanh(x) + 4 \text{sech}(x) - 2 \tanh(x) \log \{2\rho^2 \text{sech}^2(x)\} - 4x \right] \\
I_{13}(\varepsilon) &\approx I_{13}(\varepsilon = 0) - \frac{4}{3} \varepsilon \rho \int dx \tanh^2(x) + \frac{1}{2} \varepsilon (2\alpha + v\beta) \int dx \left[ 5 \tanh(x) + 4 \text{sech}(x) \right. \\
&\quad \left. - 2 \tanh(x) \log \{2\rho^2 \text{sech}^2(x)\} - 4x \right] + \frac{1}{2} \varepsilon \frac{v}{\rho} \int dx x \left[ 5 \tanh(x) + 4 \text{sech}(x) \right. \\
&\quad \left. - 4x - \underline{2 \tanh(x) \log \{2\rho^2 \text{sech}^2(x)\}} \right]. \tag{39}
\end{aligned}$$

In the second equation above the last integral (underlined) does not have any known closed mathematical form. However, this term and the similar integrals elsewhere in the above die off really fast asymptotically ( $x \rightarrow \infty$ ) as  $\text{sech}(x) \rightarrow 1$ . Since we are dealing with quasi-integrable systems whose asymptotic behavior are of practical interest, we can safely neglect such contributions. The remaining integrals, with  $x \in [X, -\rho\beta]$ , which are not expressed in Eq.s 34 are:

$$\begin{aligned}
\int dx \tanh^2(x) &= x - \tanh(x) + \text{Const.} \\
\int dx \text{sech}(x) &= 2 \arctan \left[ \tanh \left( \frac{x}{2} \right) \right] + \text{Const.} \\
\int dx \tanh(x) \log \{2\rho^2 \text{sech}^2(x)\} &= -\frac{1}{4} \log^2 [2\rho^2 \text{sech}^2(x)] + \text{Const.} \\
\int dx x \text{sech}(x) &= -i \text{Li}_2(-ie^{-x}) + i \text{Li}_2(ie^{-x}) - 2x \cot^{-1}(e^x) + \text{Const.} \tag{40}
\end{aligned}$$

## C Integrals for Nonholonomic NLS Case

In order to calculate the effect of NHD on the IHM of NLS system, the smallness of the NHD parameters ( $\rho'$  and  $v'$ ) in comparison to the undeformed parameters ( $\rho$  and  $v$ ) can be exploited so that all terms bi-linear or of higher order in  $\rho'$  and  $v'$  are neglected. This effects the simplifications:



$$\begin{aligned}\kappa &\approx 2\rho^2 \operatorname{sech}^2 \{\rho(s - \beta)\} \left[ 1 + 2\frac{\rho'}{\rho} - 2\{\rho'(s - \beta) - \rho v't\} \tanh \{\rho(s - \beta)\} \right], \\ \tau &\approx \frac{d}{dx} [2\alpha + vs + 4\rho\rho't - vv't + v's].\end{aligned}\quad (41)$$

From Eq. 11 the Hasimoto parameters can now be expressed as,

$$\begin{aligned}a &\approx 2(\rho + \rho') \tanh \{\rho(s - \beta)\} + 2\rho(\rho's - \rho'\beta - \rho v't) \operatorname{sech}^2 \{\rho(s - \beta)\}, \\ b &\approx 2\alpha + vs + 4\rho\rho't - vv't + v's \quad \text{and thus} \\ c &\approx 2\sqrt{\theta^2 + \phi^2}, \quad \text{where} \\ \phi^2 &= \frac{1}{2}(2\alpha + vs)(4\rho\rho't - vv't + v's) + 2\rho^2(\rho's - \rho'\beta - \rho v't) \tanh \{\rho(s - \beta)\} \operatorname{sech}^2 \{\rho(s - \beta)\} \\ &\quad + 2\rho\rho' \tanh^2 \{\rho(s - \beta)\}.\end{aligned}\quad (42)$$

Subsequently the nonholonomically deformed relevant IHM matrix elements, corresponding to the choice in Eq. 14, are,

$$\begin{aligned}M_{12}^d &\approx M_{12} - \frac{4}{3}\rho\phi^2 \tanh \{\rho(s - \beta)\} + 2\rho' \left( 1 - \frac{2}{3}\theta^2 \right) \tanh \{\rho(s - \beta)\} + 2\rho(\rho's - \rho'\beta - \rho v't) \operatorname{sech}^2 \{\rho(s - \beta)\}, \\ M_{13}^d &\approx M_{13} - \frac{1}{3}\rho(2\alpha + vs)\phi^2 \tanh \{\rho(s - \beta)\} + \rho'(2\alpha + vs) \left( 1 - \frac{\theta^2}{3} \right) \tanh \{\rho(s - \beta)\} \\ &\quad + 2\rho(v's + 4\rho\rho't - vv't) \tanh \{\rho(s - \beta)\} + 2\rho(2\alpha + vs)(\rho's - \rho'\beta - \rho v't) \operatorname{sech}^2 \{\rho(s - \beta)\}\end{aligned}\quad (43)$$

where  $M_{12,13}$  are the undeformed matrix elements of Eq. 15. Analogously, the integrals

$$I_{12}^d = \int_0^s M_{12}^d(s', t) ds' \quad \text{and} \quad I_{13}^d = \int_0^s M_{13}^d(s', t) ds', \quad (44)$$

will directly yield the nonholonomically deformed Frenet-Serret coordinates. In detail these integrals take the forms:

$$\begin{aligned}I_{12}^d &\approx I_{12} + \frac{\rho'}{\rho}x^2 - 2\rho v'tx - \rho\beta(\rho'\beta + 2\rho v't) - \left[ \frac{\rho'}{2\rho}\gamma^2 + \frac{2}{3}\gamma\eta' - 2\frac{\rho'}{\rho} \right] \int \tanh(x) \\ &\quad - \frac{2}{3\rho} \left[ v\frac{\rho'}{\rho}\gamma + v'\gamma + v\eta' \right] \int x \tanh(x) - \frac{v}{3\rho^3}(2\rho v' + \rho'v) \int x^2 \tanh(x) + 2\rho v't \left( 1 + \frac{4}{3}\rho^2 \right) \int \tanh^2(x) \\ &\quad - 2\frac{\rho'}{\rho} \left( 1 + \frac{4}{3}\rho^2 \right) \int x \tanh^2(x) - 4\rho\rho' \int \tanh^3(x) - \frac{8}{3}\rho^3 v't \int \tanh^4(x) + \frac{8}{3}\rho\rho' \int x \tanh^4(x),\end{aligned}\quad (45)$$

and

$$\begin{aligned}I_{13}^d &\approx I_{13} + \frac{2v\rho'}{3\rho^2}x^3 + \left( \frac{\rho'}{\rho}\gamma - vv't \right) x^2 - 2\rho\gamma v'tx - \left[ \rho\beta(\rho'\beta + 2\rho v't)\gamma - \rho^2\beta^2 vv't - \frac{2}{3}v\beta^3\rho\rho' \right] \\ &\quad - \frac{1}{12} \left[ \frac{\rho'}{\rho}\gamma^3 + 2\eta'\gamma^2 - 12\frac{\rho'}{\rho}\gamma - 24\eta' \right] \int \tanh(x) \\ &\quad - \frac{1}{6\rho} \left[ \left( \frac{3\rho'}{2\rho}v + v' \right) \gamma^2 + 2v\rho'\gamma - 12v' - 6\frac{\rho'}{\rho}v \right] \int x \tanh(x) \\ &\quad - \frac{v}{6\rho^2} \left[ \left( \frac{3\rho'}{2\rho}v + 2v' \right) \gamma + v\eta' \right] \int x^2 \tanh(x) - \frac{v^2}{12\rho^4}(v\rho' + 2\rho v') \int x^3 \tanh(x) + 2\rho v't \left( 1 + \frac{\rho^2}{3} \right) \gamma \int \tanh^2(x) \\ &\quad - 2 \left( 1 + \frac{\rho^2}{3} \right) \left[ \frac{\rho'}{\rho}\gamma - vv't \right] \int x \tanh^2(x) - \frac{2v\rho'}{\rho^2} \left( 1 + \frac{\rho^2}{3} \right) \int x^2 \tanh^2(x) - \gamma\rho\rho' \int \tanh^3(x) \\ &\quad - v\rho' \int x \tanh^3(x) - \frac{2}{3}\rho^3 v't\gamma \int \tanh^4(x) + \frac{2}{3}\rho^2 \left( \frac{\rho'}{\rho}\gamma - vv't \right) \int x \tanh^4(x) + \frac{2}{3}v\rho' \int x^2 \tanh^4(x),\end{aligned}$$

where  $\eta' = 4\rho\rho't - vv't + v'\beta$ .

In the above,  $I_{12,13}$  are the undeformed counterparts given in Eq.s 32 and 36. The values of the exact integrals in the above are already given in Eq.s 34, 37 and 40 apart from the following ones (in the indefinite form):

$$\begin{aligned}
\int x \tanh^2(x) &= \frac{x^2}{2} - x \tanh(x) + \log \{ \cosh(x) \} + \text{Const.}, \\
\int x^2 \tanh^2(x) &= \frac{x}{3} [x(x+3) + 6 \log(1 + e^{-2x}) - 3x \tanh(x)] - \text{Li}_2(-e^{-2x}) + \text{Const.}, \\
\int \tanh^4(x) &= x - \tanh(x) - \frac{1}{3} \tanh^3(x) + \text{Const.}, \\
\int x \tanh^4(x) &= \frac{1}{6} + \frac{x^2}{2} - x \tanh(x) - \frac{1}{6} \tanh^2(x) + \frac{4}{3} \log \{ \cosh(x) \} - \frac{1}{3} x \tanh^3(x) + \text{Const.}, \\
\int x^2 \tanh^4(x) &= \frac{1}{3} [x(1 + 4x + x^2) - (1 + 3x^2) \tanh(x) - x \tanh^2(x) - x^2 \tanh^3(x) + 8x \log(1 + e^{-2x}) \\
&\quad - 4\text{Li}_2(-e^{-2x})] + \text{Const.}. \tag{46}
\end{aligned}$$

## References

- [1] R. J. Baxter, *Exactly solved models in statistical mechanics* (Academic Press, London, 1982).
- [2] L. S. Da Rios, *Rend. Circ. Mat. Palermo* **22**, (1906) 117.
- [3] R. Betchov, *J. Fluid Mech.* **22**, (1965) 471.
- [4] M. Lakshmanan, *Phys. Lett. A* **61**, (1977) 53.
- [5] R. Hasimoto, *J. Fluid Mechanics* **51**, (1972) 477.
- [6] A. Majda and A. Bertozzi, *Vorticity and Incompressible Flow* (Cambridge Univ. Press, Cambridge, 2002).
- [7] L. A. Ferreira, G. Luchini G. and W. J. Zakrzewski, *The Concept of Quasi-Integrability*, *Nonlinear and Modern Mathematical Physics*, AIP Cof. Proc., **1562** (2013) 43.
- [8] L. A. Ferreira, G. Luchini and W. J. Zakrzewski, *The concept of quasi-integrability for modified non-linear Schrödinger models*, *J. High Energ. Phys.* **1209** (2012) 103.
- [9] O. Krupková, *J. Math. Phys.* **38**, (1997) 5098.
- [10] A. Kundu, *J. Phys. A: Math. Theor.* **41**, (2008) 495201 and references therein.
- [11] P. Guha, *Nonholonomic deformation of generalized KdV-type equations*, *J. Phys. A: Math. Theor.* **42**, (34), 345201.
- [12] B.K. Shivamoggi, *Eur. Phys. J. B* **86** (2013) 275.
- [13] R. A. Van Gorder, *Phys. Rev. E* **91** (2015) 053201.
- [14] K. Abhinav and P. Guha, *Inhomogeneous Heisenberg spin chain and quantum vortex filament as non-holonomically deformed NLS systems*, *Eur. Phys. J. B* **91** (2018) 52.
- [15] K. Abhinav, P. Guha and I. Mukherjee, *Study of quasi-integrable and non-holonomic deformation of equations in the NLS and DNLS hierarchy*, *J. Math. Phys.* **59**, (2018) 101507.
- [16] A. Sym, *Fluid Dyn. Res.* **3**, (1988) 151.
- [17] H. Aref and E.P. Flinchem, *J. Fluid Mech.* **148**, (1984) 477.
- [18] R. Shah, *Rogue waves on a vortex filament*, Masters thesis, University of Oxford [<https://eprints.maths.ox.ac.uk/1904/>].
- [19] C. Herring and C. Kittle, *Phys. Rev.* **81**, (1951) 869.
- [20] A. Kundu, *Nonlinearizing linear equations to integrable systems including new hierarchies with non-holonomic deformations*, *J. Math. Phys.* **50**, 102702 (2009).
- [21] O. Krupková, *J. Math. Phys.* **38**, (1997) 5098.
- [22] M. Gürses and A Peckan, *Nonlocal nonlinear Schrödinger equations and their soliton solutions*, *J. Math. Phys.* **59**, (2018) 051501.